arXiv:2110.14302v2 [hep-ph] 15 Apr 2022

Incomplete electromagnetic response of hot QCD matter

Zeyan Wang[a], Jiaxing Zhao[a], Carsten Greiner[b], Zhe Xu[a], and Pengfei Zhuang[a]
[a] *Department of Physics, Tsinghua University, Beijing 100084, China and*
[b] *Institut für Theoretische Physik, Johann Wolfgang Goethe-Universität Frankfurt, Max-von-Laue-Strasse 1, 60438 Frankfurt am Main, Germany*

(Dated: April 18, 2022)

The electromagnetic response of hot QCD matter to decaying external magnetic fields is investigated. We examine the validity of Ohm's law and find that the induced electric current increases from zero and relaxes towards the value from Ohm's law. The relaxation time is larger than the lifetime of the external magnetic field for the QCD matter in relativistic heavy-ion collisions. The lower than expected electric current significantly suppresses the induced magnetic field and makes the electromagnetic response incomplete. We demonstrate the incomplete electromagnetic response of hot QCD matter by calculations employing the parton transport model combined with the solution of Maxwell's equations. Our results show a strong suppression by two orders of magnitude in the magnetic field, relatively to calculations assuming the validity of Ohm's law. This may undermine experimental efforts to measure magnetic-field-related effects in heavy-ion collisions.

Noncentral relativistic heavy-ion collisions can generate a very strong magnetic field. Theoretical studies showed that its maximum value can reach $5m_\pi^2 \approx 10^{18}$G in Au+Au collisions at the top energy of RHIC and almost $70m_\pi^2 \approx 10^{19}$G in Pb+Pb collisions at LHC energies [1–4], where m_π is the pion mass. The symmetry and phase structure of quantum chromodynamics (QCD) are dramatically affected by strong magnetic fields [5–10]. Experimentally, the strong electromagnetic fields give rise to searching for fantastic phenomena such as the chiral magnetic effect [11–14]. Furthermore, electromagnetic field-related phenomena such as the splitting of D and $\bar{D}$ directed flow [15–19], spin polarized difference between Λ and $\bar{\Lambda}$ [20–23], and photon involved QED (quantum electrodynamics) and QCD processes [24–28] have been intensively investigated by experimental and theoretical scientists.

However, it is hard to find the fingerprint of the electromagnetic fields from the measured observables. This may lie on the weak signal of spin-related quantum fluctuations or the short lifetime of the electromagnetic fields. How the electromagnetic fields evolve in relativistic heavy-ion collisions is a basic question for studying electromagnetic effects on the QCD matter and thus, attracts great attention and broad interests [29–37].

The essential issue is the electromagnetic response of the QCD matter to the fast decay of the external electromagnetic field caused by the spectators. A Faraday current $\mathbf{j}$ will induce a magnetic field in the same direction as the external magnetic field, which prolongs the lifetime of the total magnetic field, known as Lenz's law. Usually, people used Ohm's law $\mathbf{j}^{Ohm} = \sigma_{el}(\boldsymbol{E} + \boldsymbol{V} \times \boldsymbol{B})$ to calculate the induced magnetic field. σ_{el} is the electrical conductivity and $\boldsymbol{V}$ is the hydrodynamic velocity of the QGP [3]. However, the buildup of $\mathbf{j}$ will need some time to relax to $\mathbf{j}^{Ohm}$. During this period, the induced magnetic field cannot be so large as expected so far [4, 29]. We call this as incomplete electromagnetic response, which has been overlooked in earlier studies.

The incomplete electromagnetic response might be unremarkable for matter with large spatial and timescales. The QCD matter produced in heavy-ion collisions is very special because of its small spatial and time scale. The lifetime of the external electromagnetic field is $R_A/\gamma \lesssim 0.06$ fm/c at top RHIC and LHC energies [3, 4, 38]. The average creation time of QGP is about 0.6 fm/c as utilized in numerous studies [39, 40]. If the relaxation time of $\mathbf{j}$ for reaching Ohm's law, denoted as τ_j, is comparable with or even larger than these timescales, the incomplete electromagnetic response will become significant.

Before we present numerical calculations to demonstrate the incomplete electromagnetic response of QCD matter, we estimate the relaxation time τ_j of the electric current in ϕ direction on the $x-z$ plane with the help of the Drude model. This electric current induces a magnetic field in the y direction. According to the Drude model, the change of particle momentum is caused by the Lorentz force and collisions with other particles. The Lorentz force accelerates the collective motion, while collisions resist the acceleration. The counterbalance will lead to the electric current obeying Ohm's law. The generation of the electric current is a non-Markovian process. During dt, the probability of a collision is dt/τ_m, where τ_m is the mean time between two subsequent collisions. For a particle with momentum p, the change after a collision is a fraction of p, $\Delta p \approx -p/\alpha$ on average. Then, the mean change of momentum of a quark in ϕ direction on the $x-z$ plane is

$$d\langle p_\phi\rangle(t) = -\frac{dt}{\tau_m\alpha}\langle p_\phi\rangle(t) + q_i E_\phi dt\,, \tag{1}$$

where q_i is the electric charge of the quark species. We neglect the contribution of $\boldsymbol{V} \times \boldsymbol{B}$, since it is much smaller than $\boldsymbol{E}$ near midrapidity. We have also $j_\phi^{Ohm} \approx \sigma_{el}E_\phi$. The electric current is approximately $j_\phi \approx \sum_i q_i n_i \langle p_\phi\rangle/\langle E\rangle$, where n_i is the particle number density and the averaged energy is $\langle E\rangle = 3T$. Equation (1) is rewritten in the form

$$\frac{d}{dt}\frac{j_\phi(t)}{j_\phi^{Ohm}} = -\frac{1}{\tau_m\alpha}\frac{j_\phi(t)}{j_\phi^{Ohm}} + \frac{\sum_i q_i^2 n_i}{3T\sigma_{el}}\,. \tag{2}$$

Suppose the solution has a relaxation form

$$\frac{j_\phi(t)}{j_\phi^{Ohm}} = 1 - e^{-t/\tau_j}\,. \tag{3}$$

We have then

$$\tau_j = \tau_m \alpha = \frac{3T\sigma_{el}}{\sum_i q_i^2 n_i} \sim \sigma_{el}/T^2\,. \tag{4}$$

The electrical conductivity of QCD matter has been studied by perturbative QCD [41], lattice QCD [42–48], effective models [49, 50], as well as transport approaches [51–54]. Their results of σ_{el}/T is between 0.001 and 0.4 and thus differ greatly by two orders of magnitude, see also Ref. [17]. For a typical choice of $\sigma_{el}/T = 0.03$ and temperature $T = 255$ MeV of the QGP [29], Eq. (4) gives $\tau_j = 1.12$ fm/c for two-quark flavors. This time scale is larger than the lifetime of the external electromagnetic field as well as the formation time of the QGP. We expect that the incomplete electromagnetic response of the QGP will be significant and cannot be ignored. In the following we demonstrate this incomplete electromagnetic response of QCD matter within kinetic transport calculations.

The space-time evolution of quarks and gluons in the presence of electromagnetic fields can be expressed by the relativistic Boltzmann transport equation,

$$p^\mu \partial_\mu f_i + K^\mu \frac{\partial}{\partial p^\mu} f_i = \mathcal{C}[f_i], \tag{5}$$

where $K^\mu \equiv q_i F^{\mu\nu} p_\nu = (p_0 \boldsymbol{v}\cdot\mathbf{F}_{\rm Loz.}, p_0 \mathbf{F}_{\rm Loz.})$ is four-vector Mikowski force. $F^{\mu\nu}$ is the electromagnetic field strength tensor and $\mathbf{F}_{\rm Loz.} = q_i(\boldsymbol{v}\times\boldsymbol{B} + \boldsymbol{E})$ is the Lorentz force. $\boldsymbol{v} = \boldsymbol{p}/p_0$ is the particle velocity. $\mathcal{C}[f_i]$ stands for the collision term.

The total electromagnetic fields are the sum of the external fields and the one from the responding medium. The latter is also the sum over all the electromagnetic fields from moving quarks. For a particular quark as a source, the electromagnetic fields from it can be obtained from the Liénard-Wiechert potential

$$e\boldsymbol{E}_i(\boldsymbol{r},t) = \frac{e^2}{4\pi} q_i \left(\frac{\boldsymbol{n}_s - \boldsymbol{\beta}_s}{\gamma^2 (1-\boldsymbol{\beta}_s\cdot\boldsymbol{n}_s)^3 |\boldsymbol{r}-\boldsymbol{r}_s|^2} + \frac{\boldsymbol{n}_s \times \left((\boldsymbol{n}_s - \boldsymbol{\beta}_s)\times \dot{\boldsymbol{\beta}}_s\right)}{(1-\boldsymbol{\beta}_s\cdot\boldsymbol{n}_s)^3 |\boldsymbol{r}-\boldsymbol{r}_s|} \right)_{tr}, \tag{6}$$

$$e\boldsymbol{B}_i(\boldsymbol{r},t) = \frac{e^2}{4\pi} q_i \left(\frac{\boldsymbol{\beta}_s \times \boldsymbol{n}_s}{\gamma^2 (1-\boldsymbol{\beta}_s\cdot\boldsymbol{n}_s)^3 |\boldsymbol{r}-\boldsymbol{r}_s|^2} + \frac{\boldsymbol{n}_s \times \left(\boldsymbol{n}_s \times \left((\boldsymbol{n}_s - \boldsymbol{\beta}_s)\times \dot{\boldsymbol{\beta}}_s\right)\right)}{(1-\boldsymbol{\beta}_s\cdot\boldsymbol{n}_s)^3 |\boldsymbol{r}-\boldsymbol{r}_s|} \right)_{tr}, \tag{7}$$

where "tr" means that except for $\mathbf{r}$ and t, the other quantities are evaluated at the retarded time $t_s = t - |\boldsymbol{r}-\boldsymbol{r}_s|$. $\boldsymbol{r}_s$ is the particle position at t_s. $\boldsymbol{n}_s = (\boldsymbol{r}-\boldsymbol{r}_s)/|\boldsymbol{r}-\boldsymbol{r}_s|$ denotes the unit vector pointing in the direction from the source. $\boldsymbol{\beta}_s = \boldsymbol{v}(t_s)/c$, γ is the Lorentz factor and $\dot{\boldsymbol{\beta}}_s$ is the derivative with respect to t.

Since the mass of u and d quarks is $m_q = 3$ MeV, v is nearly equal to c. At certain space-time points, the electromagnetic fields are huge for tiny $(1-\boldsymbol{\beta}_s\cdot\boldsymbol{n}_s)^3$ in the denominators in Eqs. (6) and (7). Therefore, large fluctuations of electromagnetic fields will appear in one single heavy-ion collision. By averaging a huge number of collision events one could obtain a visible response of QGP to the decaying external fields. For numerical calculations in this work, we make an approximation to take out fluctuations of the electromagnetic fields, as we replace the velocity of the moving quark $\boldsymbol{v}$ in Eqs. (6) and (7) by $\bar{\boldsymbol{v}}$, the local average velocity of the same species of quark as the source quark. By comparing the approximate and the exact results that are the convolution of Eqs. (6) and (7) with a thermal distribution function, we find that the approximation will lower the electromagnetic fields by a factor of $1-1.5$ at $T = 0.255$ GeV depending on values of $\bar{\boldsymbol{v}}$ and $\boldsymbol{r}$.

Collisions of quarks and gluons are calculated by employing the parton cascade model Boltzmann Approach of MultiParton Scatterings (BAMPS) [55], in which the scattering probabilities in each spatial cell and at each time step, derived from the collision term, are treated in a stochastic way and the test particle method is used to enhance the statistics. In addition, the change of momentum of quarks due to the Lorentz force is done within each time step [56].

Although the electrical conductivity was calculated within BAMPS including all binary and radiation processes of partons [52], in this work we assume binary collisions with constant isotropic cross section. In this case, there is a simple relationship between the electrical conductivity and the total cross section according to the relaxation-time approximation [51–54], namely,

$$\sigma_{el} = \frac{1}{3T}\tau \sum_i q_i^2 n_i\,, \tag{8}$$

where τ is the relaxation time for a slight deviation from equilibrium. Comparing Eq. (8) with Eq. (4) we obtain $\tau_j = \tau$. For binary collisions with constant isotropic cross sections we have $\tau = 1/\sum_i n_i \sigma_t$ with $\sigma_t = 2\sigma_{22}/3$ [57]. σ_{22} is the total cross section. By varying the total cross section we can see different electromagnetic response to the external fields. Qualitatively, we see from Eq. (8) that the electrical conductivity is inversely proportional to the total cross section. The smaller the cross section, the larger is the electrical conductivity and thus, the more significant would be the electromagnetic response. On the other hand, the smaller the cross section, the larger is the relaxation time for the induced electric current to reach Ohm's law. The electromagnetic response will be suppressed. In the following we present quantitative results from numerical calculations.

For our study we assume equilibrium states of gluons and quarks with u, d two flavors. Quarks and glu-

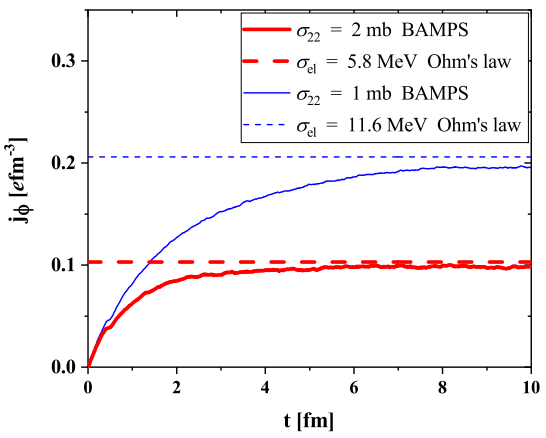


FIG. 1. The electric current density along the ϕ direction at $r = 2.5$ fm. Solid curves are the results from BAMPS calculations, while the dashed lines are the results from Ohm's law $j_\phi^{Ohm} = \sigma_{el} E_\phi$. The total cross section is set to be 1 or 2 mb.

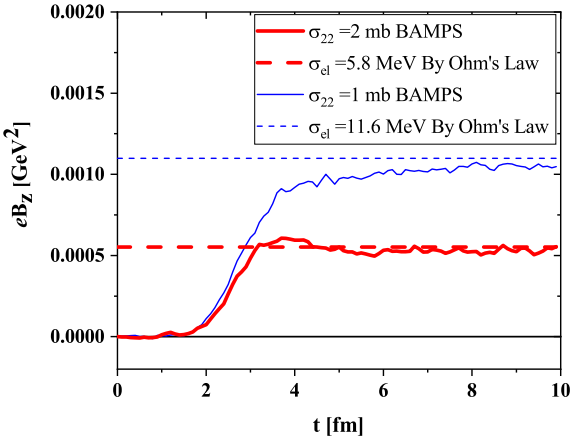


FIG. 2. The induced magnetic field at $\mathbf{r} = 0$. The solid curves are the results from BAMPS calculations, while the dashed lines are the results with Ohm's law.

ons are distributed uniformly in coordinate space and by the Boltzmann distribution function in momentum space. The temperature of the system is set to be $T = 255$ MeV. These setups lead to $\sigma_{el} = 11.6/(\sigma_{22}/\text{mb})$ MeV. We use $\sigma_{22} = 1$ and 2 mb, which correspond to $\sigma_{el} = 11.6$ and 5.8 MeV. In these cases, the shear viscosity to entropy density ratio [58, 59] is $\eta/s = 0.44$ and 0.22, respectively.

At first, we consider a linearly attenuated magnetic field as the external field, $e\boldsymbol{B}_{ex}(t) = (0.1 - 0.01t/\text{fm})\,\mathbf{e}_z\,\text{GeV}^2$, which induces an electric field $e\boldsymbol{E}(r) = (0.005r/\text{fm})\,\mathbf{e}_\phi\,\text{GeV}^2$. Such fields can be generated from an infinitely long solenoid by linearly decreasing the electric current twined around it. In our simulation, we consider a cylinder with a radius of 3 fm and a length of 6 fm. The thermal quark-gluon system is embedded in the cylinder and initialized at time 0 fm/c. A periodic boundary condition is taken in the z direction, while particles are reflected at the wall in the r direction. For this condition, the collective motion can only be in the ϕ direction. The radial motion due to the Lorentz force and the reflection from the wall cancel each other out.

The induced electric field generates an electric current. The electric current density at a radius r is calculated by

$$j_\phi(t) = \frac{1}{V}\sum_i q_i \frac{p_\phi^i(t)}{p_0^i(t)}, \tag{9}$$

where the summation is over all quarks in the cylindrical shell within radius $[r - \Delta r/2 : r + \Delta r/2]$. V is the volume. The solid curves in Fig. 1 show the buildup of the electric current density taken at $r = 2.5$ fm with $\Delta r = 0.1$ fm. We see that the induced electric field generates a circular electric current, which is increasing from zero and relaxing towards the value from Ohm's law. Also, the relaxation time with $\sigma_{22} = 1$ mb is longer than that with $\sigma_{22} = 2$ mb, as expected. Even though, the generated electric current with $\sigma_{22} = 1$ mb is always larger than that with $\sigma_{22} = 2$ mb. The results in Fig. 1 can actually be understood by the Drude model as discussed before. For $\sigma_{22} = 1, 2$ mb, the relaxation time is $\tau_j = 1.72, 0.86$ fm/c, respectively, according to Eqs. (4) and (8). These values are just 10% smaller than the numerical results.

The electric current will generate a magnetic field denoted as the induced magnetic field, which should counteract the decay of the external magnetic field obeying Lenz's law. In Fig. 2 we show the generation of the induced magnetic field at $\mathbf{r} = 0$ by the solid curves. The dashed lines represent the results calculated with Ohm's law. Similar to the electric current, the induced magnetic field is increasing from zero and relaxing towards the values calculated with Ohm's law. The induced magnetic field at early time $t < 3$ fm/c seems independent of the total cross section or the electrical conductivity of QGP. The reason may lie in the retardation of the electromagnetic fields.

From Figs. 1 and 2 we see the agreements of the BAMPS results at late times with those from or with Ohm's law, even a little lower because of the finite length of the cylinder. These indicate that the approximation we made for the calculation of the electromagnetic fields of moving quarks is applicable. At this point, the example with a linearly decreasing external magnetic field serves as a cross-check on the additional numerical implementations.

Now we turn to another assumption of the external magnetic field, which mimics the situation in noncentral relativistic heavy-ion collisions and has been considered in Ref. [4]. In this paper two nuclei are replaced by two point particles with the same charge and mass (for a more

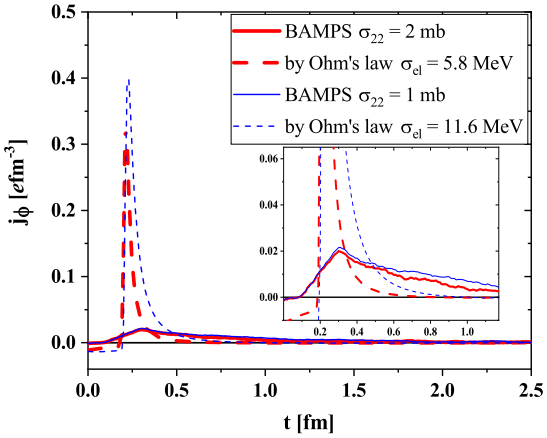


FIG. 3. The electric current density at $(x = 2\,\text{fm}, y = 0, z = 0.2\,\text{fm})$. The solid curves are the results from BAMPS, while the dashed curves are the results by solving Eqs. (10) and (11) and using Ohm's law.

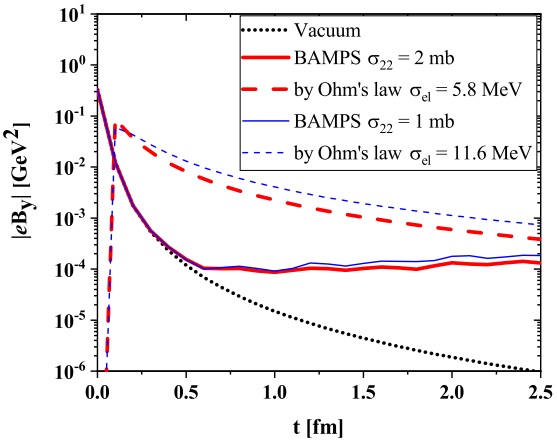


FIG. 4. The magnetic field at $\mathbf{r} = 0$ fm. The dotted curve depicts the external field, the solid curves are the total magnetic field (induced plus external field) from BAMPS calculation, and the dashed curves are the total magnetic field by solving Eqs. (10) and (11).

realistic consideration see Ref. [29]). They are moving in the z direction at impact parameter $\mathbf{b} = b\ \mathbf{e}_x$ and generate external electromagnetic fields for a quark-gluon system, which is assumed to be static, thermal and fill the whole coordinate space. The electromagnetic fields of the quark-gluon system are solved by Maxwell's equations

$$\nabla \cdot \boldsymbol{B} = 0, \nabla \times \boldsymbol{E} = -\frac{\partial \boldsymbol{B}}{\partial t}, \tag{10}$$

$$\begin{aligned} \nabla \cdot \boldsymbol{E} &= q\delta(x - b/2)\delta(y)\delta(z - vt) \\ &\quad + q\delta(x + b/2)\delta(y)\delta(z + vt)\,, \\ \nabla \times \boldsymbol{B} &= \frac{\partial \boldsymbol{E}}{\partial t} + \sigma_{el}\boldsymbol{E} \\ &\quad + qv\hat{\mathbf{z}}\delta(x - b/2)\delta(y)\delta(z - vt) \\ &\quad - qv\hat{\mathbf{z}}\delta(x + b/2)\delta(y)\delta(z + vt)\,. \end{aligned} \tag{11}$$

v denotes the velocity of the nucleus, which is $v = (1 - 4m_N^2/s)^{1/2}$. m_N is the mass of a nucleon and $\sqrt{s}$ is the colliding energy per nucleon pair. In Refs. [4, 29], the $\boldsymbol{V} \times \boldsymbol{B}$ term in Ohm's law was not taken into account. Recall that $\boldsymbol{V}$ is the hydrodynamic velocity of the QCD matter. We repeat the calculations in Ref. [4] and show results for $q = 79e$, $\sqrt{s} = 200$ GeV, $b = 7.6$ fm, and $\sigma_{el} = 5.8$ and 11.6 MeV in Figs. 3 and 4 by dashed curves.

In our calculation with BAMPS we assume that a static and thermal quark-gluon system appears at $t = 0$ fm/c, when two point-like nuclei are at the closest distance. Furthermore, the quark-gluon system is embedded in a cube with a length of 6 fm between the two nuclei. Periodic boundary conditions are used. The temperature of the quark-gluon system is set to be $T = 255$ MeV and the total cross section is $\sigma_{22} = 2$ or 1 mb, which corresponds to $\sigma_{el} = 5.8$ or 11.6 MeV. The external electromagnetic fields are calculated via Eqs. (6) and (7) for moving point-like nuclei.

When two point-like nuclei are approaching each other, the electromagnetic fields at the central region around $\mathbf{r} = 0$ fm are increasing. When the two point-like nuclei are at the closest distance (collision at $t = 0$ fm/c), the magnetic field is at the maximum. Therefore, the induced electric field disappears at this moment and is increasing again (but in opposite direction), when two point-like nuclei are departing from each other.

Figure 3 shows the electric current density at $(x = 2$ fm$, y = 0, z = 0.2$ fm$)$, generated by the total electric field. We plot the ϕ-component of the current in polar coordinate system on the $x - z$ plane, since it is responsible for the induced magnetic field in the y direction. The electric field has a strong x component. Thus, E_ϕ is almost $-E_x z/|x|$. The solid curves are the results from BAMPS calculation, while the dashed ones are obtained by solving Eqs. (10) and (11) and using Ohm's law. We see promptly increasing electric currents when explicitly using Ohm's law. The current with $\sigma_{el} = 5.8$ MeV peaks within the time window $[0.2 : 0.4$ fm/c$]$, while that with $\sigma_{el} = 11.6$ MeV peaks within $[0.2 : 0.6$ fm/c$]$. Compared with these, the results from BAMPS show almost twentyfold lower peaks with longer tails. The large difference is due to the relaxation of the electric current towards Ohm's law.

The external magnetic field is increasing before $t = 0$ fm/c. Thus, the induced magnetic field is in the opposite direction as the external field. By passing $t = 0$ fm/c, the induced electric field reverses. If the quark-gluon system exists before 0 fm/c, the induced magnetic field reverses too, but with delay due to the retardation. Therefore, after 0 fm/c the total magnetic field by solving Eqs. (10) and (11) is smaller than the external magnetic field for a while. This is shown in Fig. 4 by the dashed

curves for the total magnetic field at $\mathbf{r} = 0$ fm. The dotted curve depicts the external field. By explicitly using Ohm's law, the electromagnetic response of the quark-gluon system is much more significant. At $t = 0.5$ fm/c for instance, the induced magnetic field is larger than the external field by two orders of magnitude, although it is ten times smaller than the maximal value of the external field at $t = 0$ fm/c.

In the calculation with BAMPS, the induced magnetic field is generated after $t = 0$ fm/c. The result demonstrates the incomplete electromagnetic response. The induced magnetic field is tiny at early times. Only after $t = 0.5$ fm/c does it become dominant over the external field and stay almost constant. However, the induced magnetic field after 0.5 fm/c is smaller than the maximal field at 0 fm/c by three orders of magnitude. Such a small value may suppress any magnetic effects. Besides the incompleteness, one has to take into account the retardation of the generation of the magnetic field. From Fig. 4 we also see that the magnetic field is not sensitive to the cross section, especially from 0 to 0.5 fm/c. Even though the application of kinetic transport models for QCD medium with large coupling (large cross sections) may be in question, we do not expect a strong increase of the magnetic field after 0.5 fm/c in real heavy-ion collisions.

Some discussions are in order. The quark-gluon system we considered is an idealized one. In real heavy-ion collisions the produced quark-gluon system expands, cools, and hadronizes. The temperature decreases and the electrical conductivity of the QGP changes with time. Although all these will also influence the electromagnetic response of the QGP to the external fields, its incompleteness we proposed makes an important contribution and should be taken seriously into account. Moreover, at the early stage of heavy-ion collisions, the produced quarks and gluons are far from kinetic and chemical equilibrium [55, 60, 61]. Quark number is smaller than that at thermal equilibrium, which will lead to a smaller induced electrical current. All of these considerations can be included in a more comprehensive study by using BAMPS with more realistic initial condition and pQCD interactions. The results will be presented in a future presentation.

In summary, in this Letter we have challenged the validity of Ohm's law applied for the hot QCD matter produced at the early stage of noncentral relativistic heavy-ion collisions. We have proposed the incomplete electromagnetic response due to the relaxation of the induced electric current towards Ohm's law. The incomplete electromagnetic response of hot QCD matter to external electromagnetic fields has been demonstrated by using the parton cascade model BAMPS combined with the solution of Maxwell's equations. The numerical results showed the significant suppression of the induced magnetic field. This makes the search for any magnetic effects in heavy-ion experiments even more challenging.

This work was financially supported by the National Natural Science Foundation of China under Grants No. 11890710, No. 11890712, No. 12035006, and No. 12047535. C.G. acknowledges support by the Deutsche Forschungsgemeinschaft (DFG) through the grant CRC-TR 211 "Strong-interaction matter under extreme conditions." The BAMPS simulations were performed at Tsinghua National Laboratory for Information Science and Technology and on TianHe-1(A) at National Supercomputer Center in Tianjin.

[1] V. Skokov, A. Y. Illarionov and V. Toneev, Int. J. Mod. Phys. A **24**, 5925-5932 (2009).
[2] V. Voronyuk, V. D. Toneev, W. Cassing, E. L. Bratkovskaya, V. P. Konchakovski and S. A. Voloshin, Phys. Rev. C **83**, 054911 (2011).
[3] W. T. Deng and X. G. Huang, Phys. Rev. C **85**, 044907 (2012).
[4] K. Tuchin, Adv. High Energy Phys. **2013**, 490495 (2013).
[5] J. O. Andersen, W. R. Naylor and A. Tranberg, Rev. Mod. Phys. **88**, 025001 (2016).
[6] D. E. Kharzeev, K. Landsteiner, A. Schmitt and H. U. Yee, Lect. Notes Phys. **871**, 1-11 (2013).
[7] G. S. Bali, F. Bruckmann, G. Endrodi, Z. Fodor, S. D. Katz, S. Krieg, A. Schafer and K. K. Szabo, JHEP **02**, 044 (2012).
[8] G. S. Bali, F. Bruckmann, G. Endrodi, Z. Fodor, S. D. Katz and A. Schafer, Phys. Rev. D **86**, 071502 (2012).
[9] F. Bruckmann, G. Endrodi and T. G. Kovacs, JHEP **04**, 112 (2013).
[10] M. D'Elia, L. Maio, F. Sanfilippo and A. Stanzione, Phys. Rev. D **105**, no.3, 034511 (2022).
[11] K. Fukushima, D. E. Kharzeev and H. J. Warringa, Phys. Rev. D **78**, 074033 (2008).
[12] D. E. Kharzeev, L. D. McLerran and H. J. Warringa, Nucl. Phys. A **803**, 227-253 (2008).
[13] D. E. Kharzeev, J. Liao, S. A. Voloshin and G. Wang, Prog. Part. Nucl. Phys. **88**, 1-28 (2016).
[14] J. Zhao and F. Wang, Prog. Part. Nucl. Phys. **107**, 200-236 (2019).
[15] S. K. Das, S. Plumari, S. Chatterjee, J. Alam, F. Scardina and V. Greco, Phys. Lett. B **768**, 260-264 (2017).
[16] S. Chatterjee and P. Bozek, Phys. Lett. B **798**, 134955 (2019).
[17] J. Zhao, K. Zhou, S. Chen and P. Zhuang, Prog. Part. Nucl. Phys. **114**, 103801 (2020).
[18] J. Adam *et al.* [STAR], Phys. Rev. Lett. **123**, no.16, 162301 (2019).
[19] S. Acharya *et al.* [ALICE], Phys. Rev. Lett. **125**, no.2, 022301 (2020).
[20] L. Adamczyk *et al.* [STAR], Nature **548**, 62-65 (2017).
[21] B. Müller and A. Schäfer, Phys. Rev. D **98**, no.7, 071902 (2018).
[22] X. Guo, J. Liao and E. Wang, Sci. Rep. **10**, no.1, 2196

(2020).
[23] Y. Guo, S. Shi, S. Feng and J. Liao, Phys. Lett. B **798**, 134929 (2019).
[24] J. Adam *et al.* [ALICE], Phys. Rev. Lett. **116**, no.22, 222301 (2016).
[25] W. Zha, L. Ruan, Z. Tang, Z. Xu and S. Yang, Phys. Lett. B **789**, 238-242 (2019).
[26] S. Klein, A. H. Mueller, B. W. Xiao and F. Yuan, Phys. Rev. Lett. **122**, no.13, 132301 (2019).
[27] J. Adam *et al.* [STAR], Phys. Rev. Lett. **127**, no.5, 052302 (2021).
[28] J. D. Brandenburg, W. Zha and Z. Xu, Eur. Phys. J. A **57**, no.10, 299 (2021).
[29] U. Gursoy, D. Kharzeev and K. Rajagopal, Phys. Rev. C **89**, 054905 (2014).
[30] K. Tuchin, Phys. Rev. C **93**, 014905 (2016).
[31] B. G. Zakharov, Phys. Lett. B **737**, 262-266 (2014).
[32] S. Pu, V. Roy, L. Rezzolla and D. H. Rischke, Phys. Rev. D **93**, 074022 (2016).
[33] G. Inghirami, L. Del Zanna, A. Beraudo, M. H. Moghaddam, F. Becattini and M. Bleicher, Eur. Phys. J. C **76**, 659 (2016).
[34] L. Yan and X. G. Huang, arXiv:2104.00831 [nucl-th].
[35] E. Stewart and K. Tuchin, Phys. Rev. C **97**, no.4, 044906 (2018).
[36] E. Stewart and K. Tuchin, Nucl. Phys. A **1016**, 122308 (2021).
[37] Y. Chen, X. L. Sheng and G. L. Ma, Nucl. Phys. A **1011**, 122199 (2021).
[38] K. Hattori and X. G. Huang, Nucl. Sci. Tech. **28**, no.2, 26 (2017).
[39] B. Schenke, S. Jeon and C. Gale, Phys. Rev. C **82**, 014903 (2010).
[40] G. Kestin and U. W. Heinz, Eur. Phys. J. C **61**, 545-552 (2009).
[41] P. B. Arnold, G. D. Moore and L. G. Yaffe, JHEP **05**, 051 (2003).
[42] S. Gupta, Phys. Lett. B **597**, 57-62 (2004).
[43] G. Aarts, C. Allton, J. Foley, S. Hands and S. Kim, Phys. Rev. Lett. **99**, 022002 (2007).
[44] P. V. Buividovich, M. N. Chernodub, D. E. Kharzeev, T. Kalaydzhyan, E. V. Luschevskaya and M. I. Polikarpov, Phys. Rev. Lett. **105**, 132001 (2010).
[45] H.-T. Ding, A. Francis, O. Kaczmarek, F. Karsch, E. Laermann and W. Soeldner, Phys. Rev. D **83**, 034504 (2011).
[46] Y. Burnier and M. Laine, Eur. Phys. J. C **72**, 1902 (2012).
[47] B. B. Brandt, A. Francis, H. B. Meyer and H. Wittig, JHEP **03**, 100 (2013).
[48] A. Amato, G. Aarts, C. Allton, P. Giudice, S. Hands and J. I. Skullerud, Phys. Rev. Lett. **111**, 172001 (2013).
[49] S. I. Finazzo and J. Noronha, Phys. Rev. D **89**, 106008 (2014).
[50] P. Sahoo, S. K. Tiwari and R. Sahoo, Phys. Rev. D **98**, 054005 (2018).
[51] W. Cassing, O. Linnyk, T. Steinert and V. Ozvenchuk, Phys. Rev. Lett. **110**, 182301 (2013).
[52] M. Greif, I. Bouras, C. Greiner and Z. Xu, Phys. Rev. D **90**, 094014 (2014).
[53] A. Puglisi, S. Plumari and V. Greco, Phys. Rev. D **90**, 114009 (2014).
[54] T. Steinert and W. Cassing, Phys. Rev. C **89**, no.3, 035203 (2014).
[55] Z. Xu and C. Greiner, Phys. Rev. C **71**, 064901 (2005).
[56] M. Greif, C. Greiner and Z. Xu, Phys. Rev. C **96**, no.1, 014903 (2017).
[57] Z. Xu and C. Greiner, Phys. Rev. C **76**, 024911 (2007).
[58] T. Hirano and M. Gyulassy, Nucl. Phys. A **769**, 71-94 (2006).
[59] A. El, F. Lauciello, C. Wesp, Z. Xu and C. Greiner, Nucl. Phys. A **925**, 150-160 (2014).
[60] J. P. Blaizot, F. Gelis, J. F. Liao, L. McLerran and R. Venugopalan, Nucl. Phys. A **873**, 68-80 (2012).
[61] P. Romatschke, Phys. Rev. Lett. **120**, 012301 (2018).